The catalytic effect of water on the keto-enol tautomerism. Pyruvate and acetylacetone: a computational challenge

Giuliano Alagona,*[a] Caterina Ghio[a] and Peter I. Nagy[b]

[a] *CNR-IPCF, Molecular Modelling Lab, Via Moruzzi 1, I-56124 Pisa, Italy. Fax: +39 050 3152442; Tel: +39 050 3152450; E-mail: G.Alagona@ipcf.cnr.it*

[b] *Center for Drug Design and Development and the Department of Medicinal and Biological Chemistry, The University of Toledo, Toledo, OH, 43606-3390. Fax: 1-419-530-7946; Tel: 1-419-530-1945; E-mail: pnagy@utnet.utoledo.edu*

Electronic Supplementary Information

Table of Content

carbonyl O (–26.5/0.99); (b) best match between the optimised structure (in red) and the grid-point on the PES of Fig. 7 at –60/1.0 (in cyan).

Figure S9. (a) B3LYP/6-31G* transition state (TS) structure of dihydrated acetylacetone optimised starting from the grid point at –80/1.2 on the PES of Fig. 7. Despite located at –49.1/1.16 the structures are similar. This TS structure corresponds to a sequential mechanism, i.e. only the H_8 atom is being delivered. Subsequently H_{17} should be shuttled as well. (b) The B3LYP/6-31G* TS optimised structure starting from –60/1.2 is consistent with the nonIMHB KE in the bottom right region of Fig. 7.

Figure S10. B3LYP/6-31G* potential energy surface of the dihydrated acetylacetone tautomerism with a number of stationary points (see text).

Figure S11 B3LYP/6-31G* KK optimised structure starting from waters located in the same region of space (structure close to the top left corner of Figs. 8 and 11).

Figure S12. B3LYP/6-31G* KE optimised structure starting from the stationary point in the upper right corner of Fig. 8.

Figure S13. B3LYP/6-31G* potential energy surface resulting from a top to bottom scan (i.e. for each $O_{19}\cdots H_8$ separation, the $O_7C_5C_4C_2$ dihedral angle spans the 80 to –60° range and so on). This map is identical to that displayed in Fig. 14 (resulting from a left to right scan), but in the KE region where only the lowest minimum structure is obtained.

Figure S14. B3LYP/6-31G* optimised structure obtained moving from the KE to the KK structure (see text).

Figure S15. MP2/aug-cc-pvdz optimised structures obtained starting from the KE structure in Fig. 9: (a) front view; (b) top view.

Figure S16. Structures of the best KK tautomer in Fig. 9 optimised at several levels: (a) B3LYP/6-31G*; (b) B3LYP/6-31++G**; (c) MP2/6-31G*; (d) MP2/aug-cc-pvdz. Some geometric parameters are also reported and compared to those of the isolated KK tautomer embedded in IEF-PCM aqueous solution (displayed in Fig. S18c).

Figure S17. Structures of the KK tautomer in the top left corner of Fig. 9 optimised at two levels: (a) B3LYP/6-31G*; (b) B3LYP/6-31++G**. Some geometric parameters are also reported.

Figure S18. Optimised structures corresponding to: (a) the lowest energy KK tautomer in vacuo (B3LYP/6-31G*); (b) the lowest energy KK tautomer in water solution (IEF-PCM/B3LYP/6-31G*, 0.39 kcal/mol more stable than the (a) structure found in water solution, practically indistinguishable from that in vacuo); (c) the lowest energy KK tautomer in water solution (IEF-PCM/B3LYP/6-311++G**), used for the explicit solvent MC/FEP simulations.

Table S1. Basis set effects on the stability of pyruvate tautomer conformations.[a]

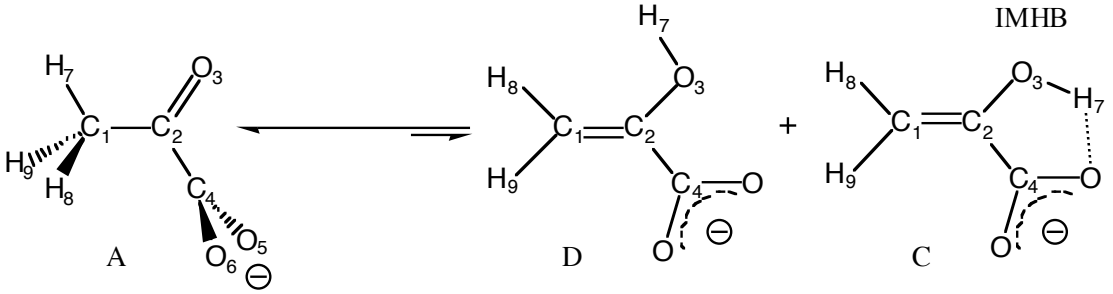

	EP		KP–EP				KP	
	C-D		A-C		A-D		A-B[b]	
B3LYP	ΔE	ΔG	ΔE	ΔG	ΔE	ΔG	ΔE	ΔG
6-31G*	-18.14	-17.03	-3.84	-5.93	-21.99	-22.97	-0.38	-1.57
6-31++G**	-16.11	-14.96	-3.48	-5.66	-19.60	-20.62	-2.35	-3.60
6-311++G**	-15.85	-14.49	-3.26	-5.55	-19.11	-20.04	-2.25	-3.57

[a] ketopyruvate (KP), A and B conformers; enolpyruvate (EP), C and D conformers; relative values in kcal/mol; [b] B (corresponding to A but for the COO^- moiety, which is in the heavy atom plane as in C and D) is a rotational transition state at all levels.

Absolute values (E_h) are:

B3LYP		A	B	C	D
6-31G*	E	–341.836516	–341.835903	–341.830391	–341.801477
	G(298)	–341.809471	–341.806972	–341.800016	–341.772871
6-31++G**	E	–341.886681	–341.882938	–341.881127	–341.855450
	G(298)	–341.860213	–341.854480	–341.851195	–341.827351
6-311++G**	E	–341.974214	–341.970627	–341.969017	–341.943753
	G(298)	–341.948065	–341.942374	–341.939218	–341.916128

Table S2. B3LYP/6-31G* relative free energy at 298 K with respect to the isolated partners for the diketo (KK) and TS structures of the dihydrated acetylacetone with the relevant TS–KK barriers[a]

PES	KK	TS	TS–KK
Fig. 7	2.00	35.89/35.87	33.89/33.87
Fig. S9	2.00	35.89	33.89
Fig. 8	0.40	20.38	19.98
Fig. 11	0.40	27.95	27.55
Fig. 9	0.16/–0.81	20.28	20.12/21.09

[a] kcal/mol; reference free energy (acetylacetone + w + w) = –498.516461 E_h.

Table S3. IEF-PCM reference values of E^{s}_{int} (as defined in eq. 2) for the keto-enol (KE) tautomer of acetylacetone at the various levels considered in Table 7.

Level	**E^{s}_{int} (E_h)**
B3LYP/6-311++G**	–345.909338
B3LYP/6-31G*//DFT[a]	–345.798472
MP2/aug-cc-pvdz//DFT	–344.868260
MP2/aug-cc-pvtz//DFT	–345.172135
CCSD(T)/aug-cc-pvdz//DFT	–344.962278
MP2/CBS//DFT	–345.300082
CCSD(T)/CBS//DFT	–345.394100
MP2/aug-cc-pvdz	–344.868692
MP2/aug-cc-pvtz//MP2[b]	–345.170640
CCSD(T)/aug-cc-pvdz//MP2	–344.963280
MP2/CBS//MP2	–345.297776
CCSD(T)/CBS//MP2	–345.392364

[a] //DFT means //B3LYP/6-311++G**, i.e. structure optimised at the B3LYP/6-311++G** level; [b] //MP2 means //MP2/aug-cc-pvdz, i.e. structure optimised at the MP2/aug-cc-pvdz level.

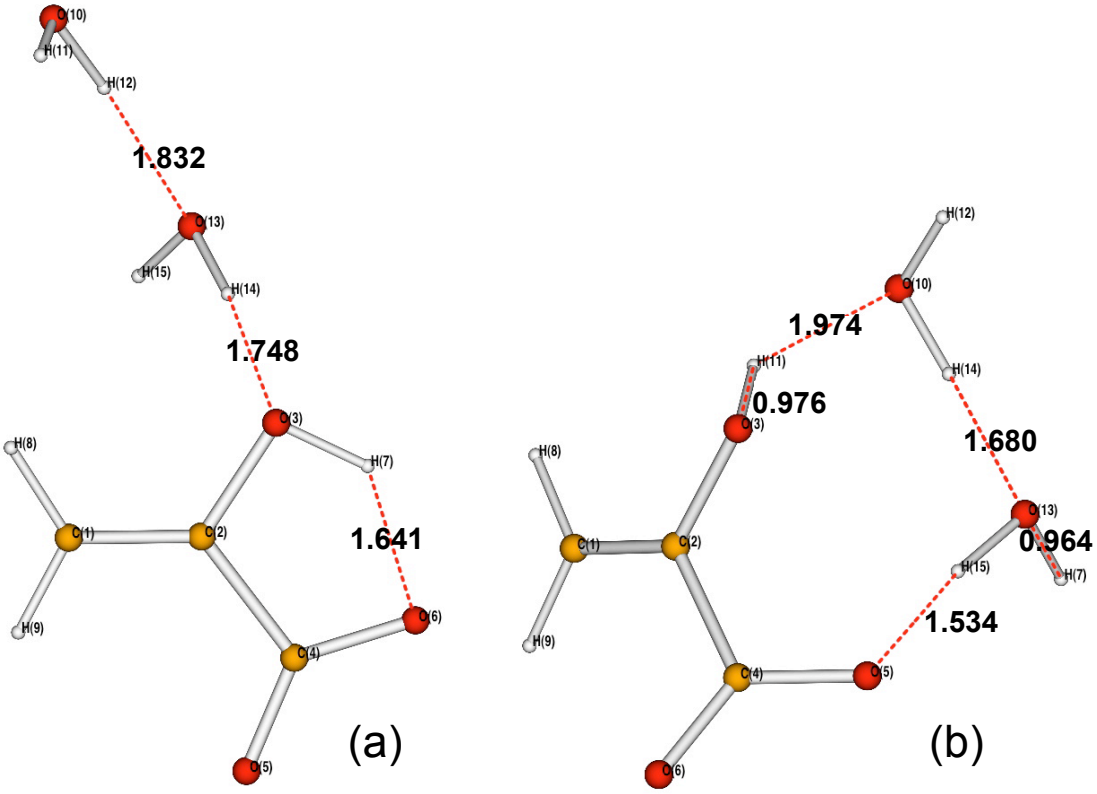

Figure S1. B3LYP/6-31++G** dihydrated structures of enolpyruvate: (a) with IMHB; (b) without IMHB.

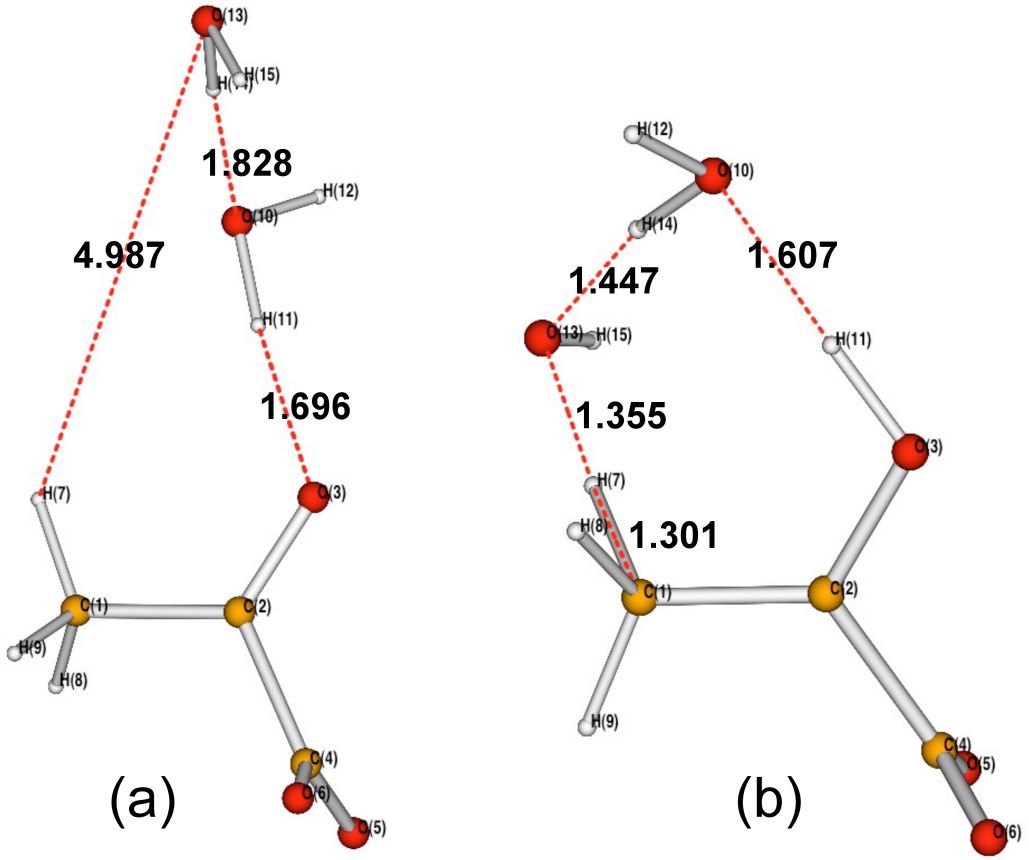

Figure S2 B3LYP/6-31++G** optimised dihydrated structures of pyruvate starting from two of the stationary points in Fig. 5: (a) keto and (b) TS.

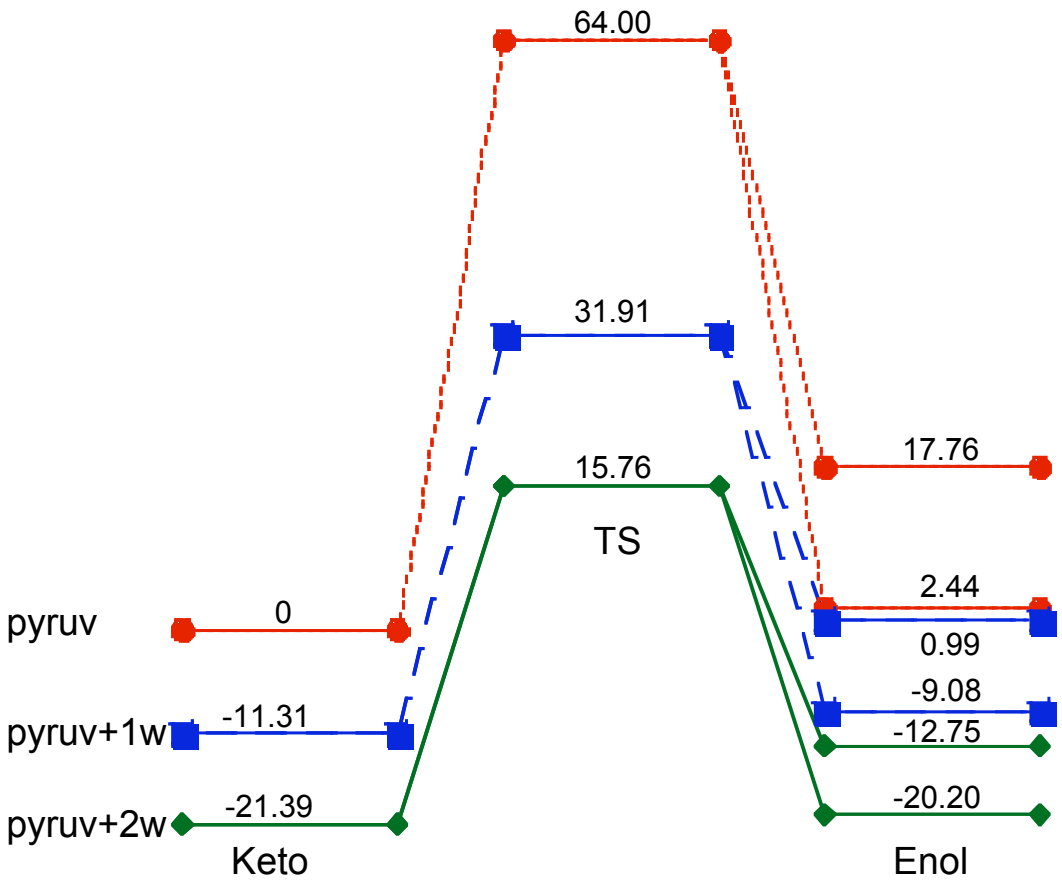

Figure S3. MP2/aug-cc-pvdz//MP2/aug-cc-pvdz potential energy profiles for the isolated, mono- and dihydrated pyruvate optimised structures at that level. For the enolpyruvate (Enol) form both the more stable intramolecularly H-bonded (IMHB) and nonIMHB structure values are reported.

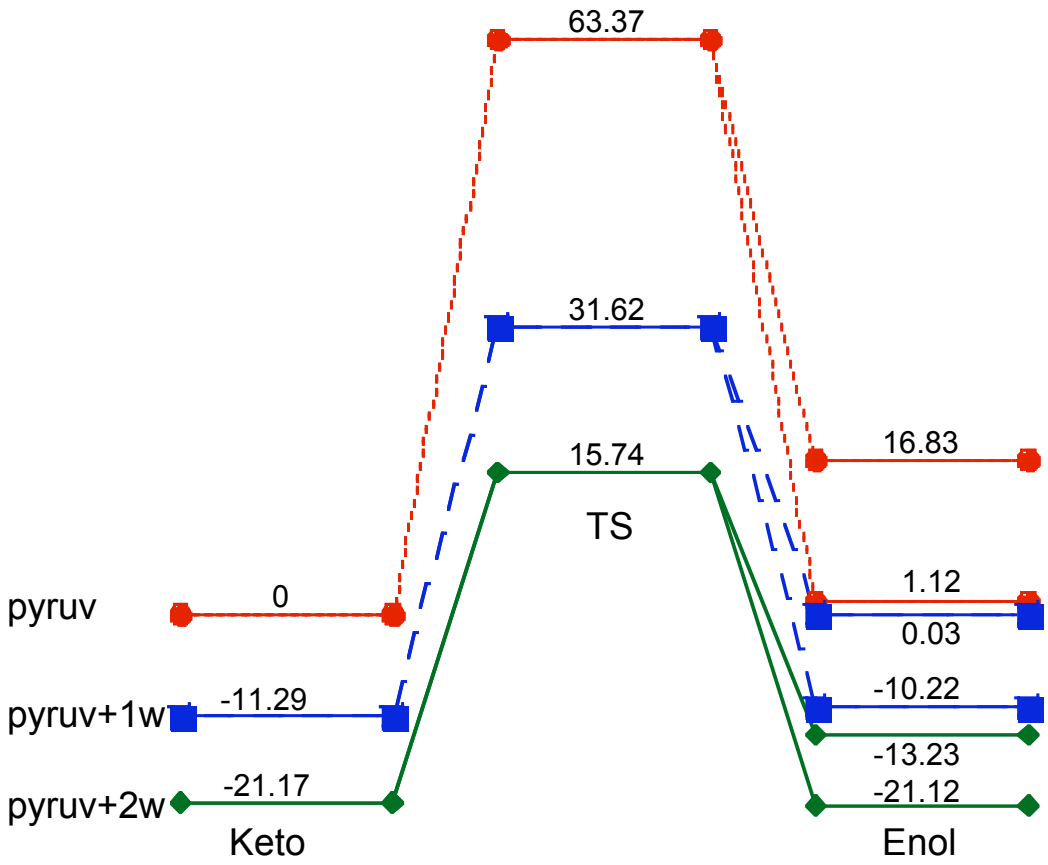

Figure S4. MP2/aug-cc-pvtz//MP2/aug-cc-pvdz potential energy profiles for the isolated, mono- and dihydrated pyruvate. The basis set effect is very limited at constant geometry. For the enolpyruvate (Enol) form both the more stable intramolecularly H-bonded (IMHB) and nonIMHB structure values are reported.

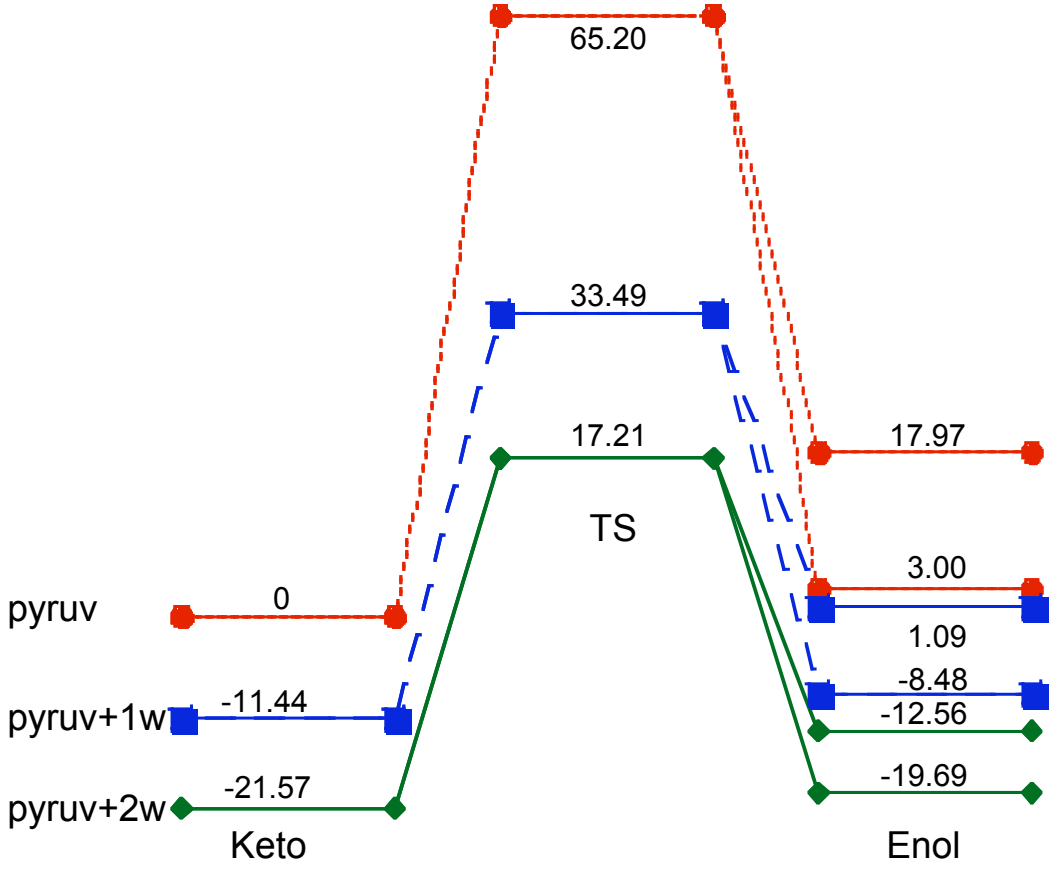

Figure S5. CCSD(T)/aug-cc-pvdz//MP2/aug-cc-pvdz potential energy profiles for the isolated, mono- and dihydrated pyruvate. For the enolpyruvate (Enol) form both the more stable intramolecularly H-bonded (IMHB) and nonIMHB structure values are reported.

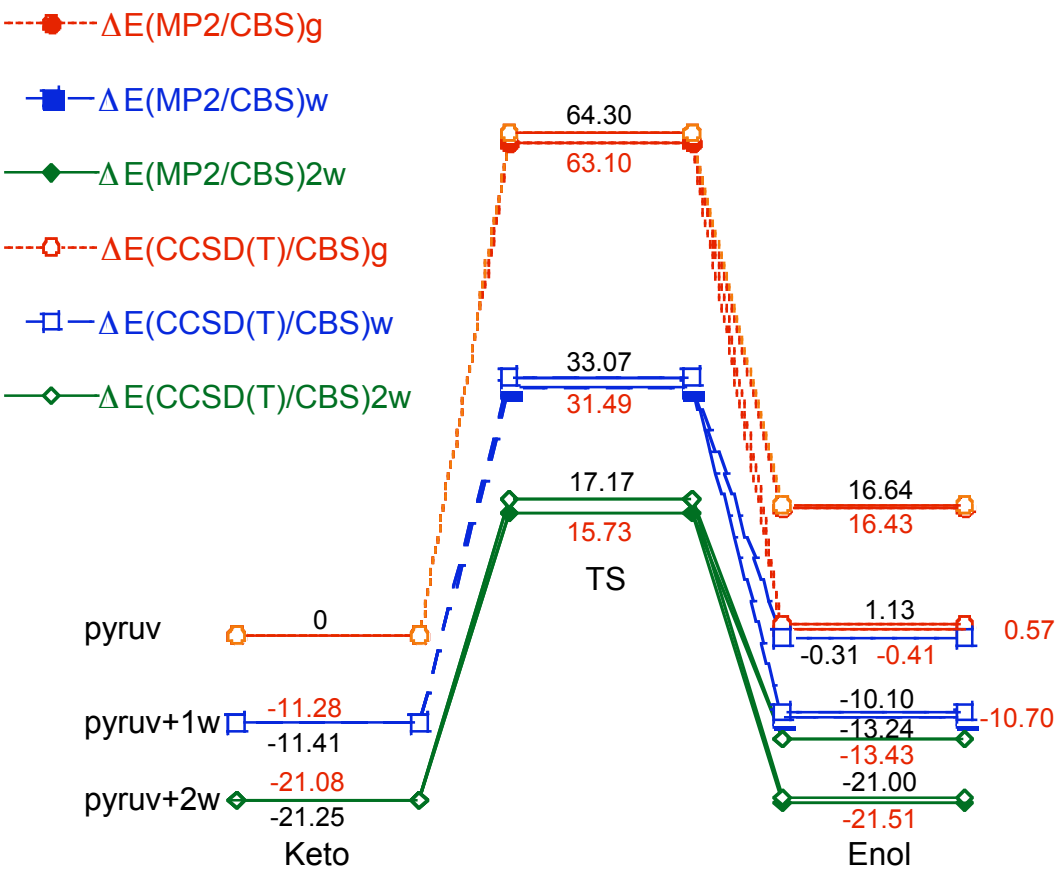

Figure S6. MP2/CBS vs CCSD(T)/CBS potential energy profiles for the isolated (g), mono- (w) and dihydrated (2w) pyruvate tautomers at the MP2/aug-cc-pvdz optimised geometries. For the enolpyruvate (Enol) form both the more stable intramolecularly H-bonded (IMHB) and nonIMHB structure values are reported.

The largest difference between the two correlated methods is found on the transition state (TS) relative energies, slightly more favourable (by 1.2-1.6 kcal/mol) at the MP2 level (numbers in red ink). For the enolpyruvate (Enol) form both the more stable intramolecularly H-bonded (IMHB) and nonIMHB structure values are reported.

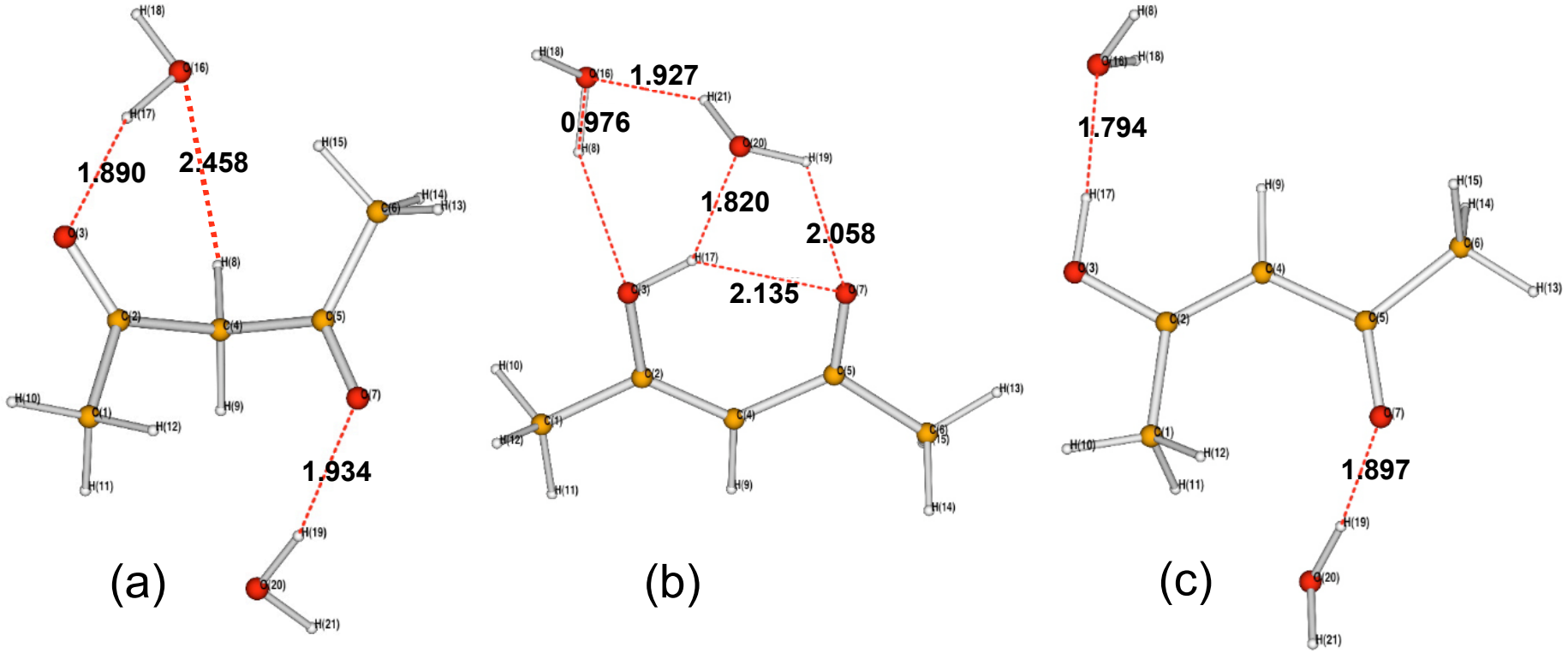

Figure S7. B3LYP/6-31G* optimised structures of dihydrated acetylacetone tautomers starting from the stationary points in Fig. 7: (a) KK, (b) and (c) KE forms.

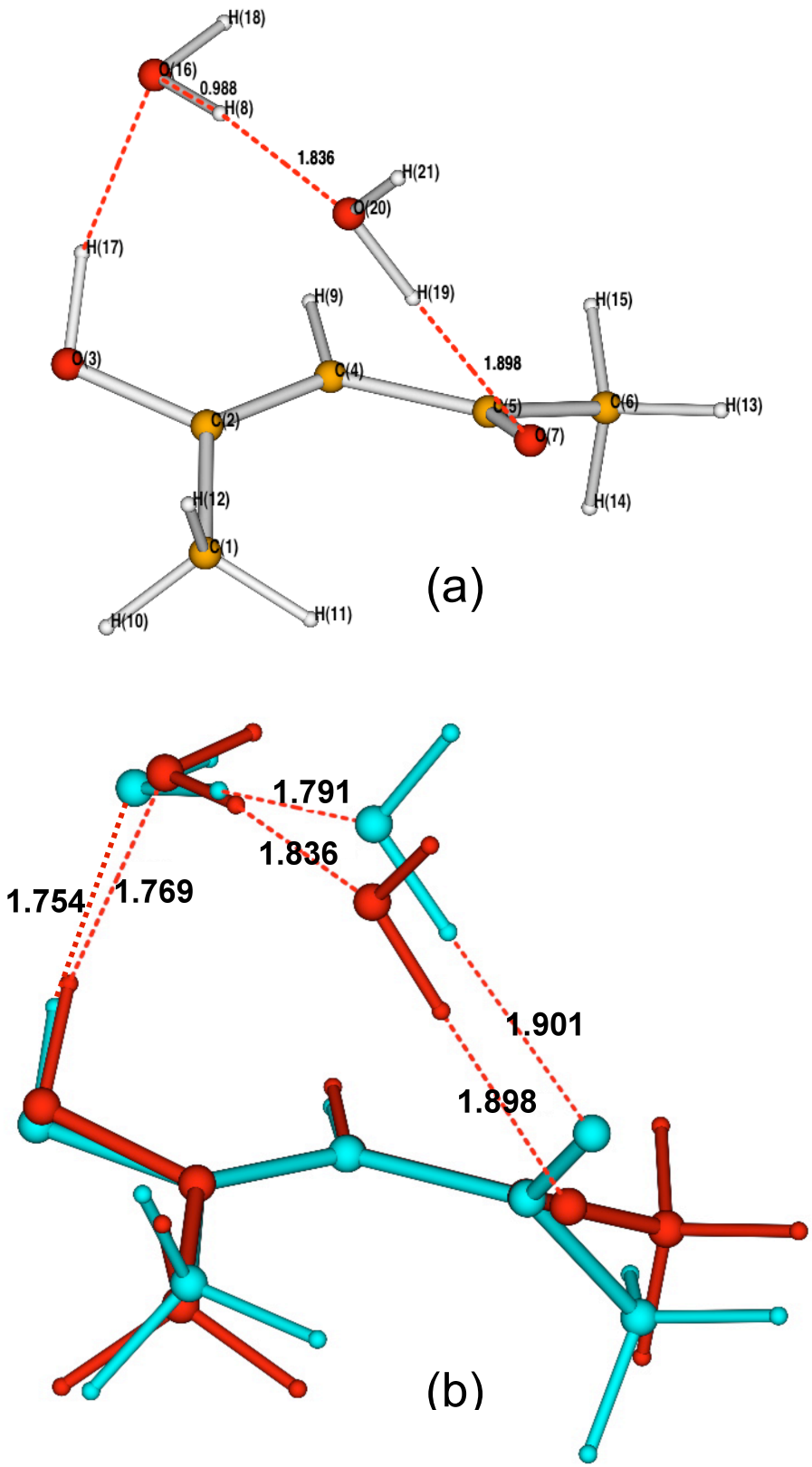

Figure S8. (a) B3LYP/6-31G* keto-enol (KE) optimised structure of dihydrated acetylacetone with the water molecules bridged between the hydroxyl H and the carbonyl oxygen (–26.5/0.99); (b) best match between the optimised structure (in red) and the grid-point on the PES of Fig. 7 at –60/1.0 (in cyan).

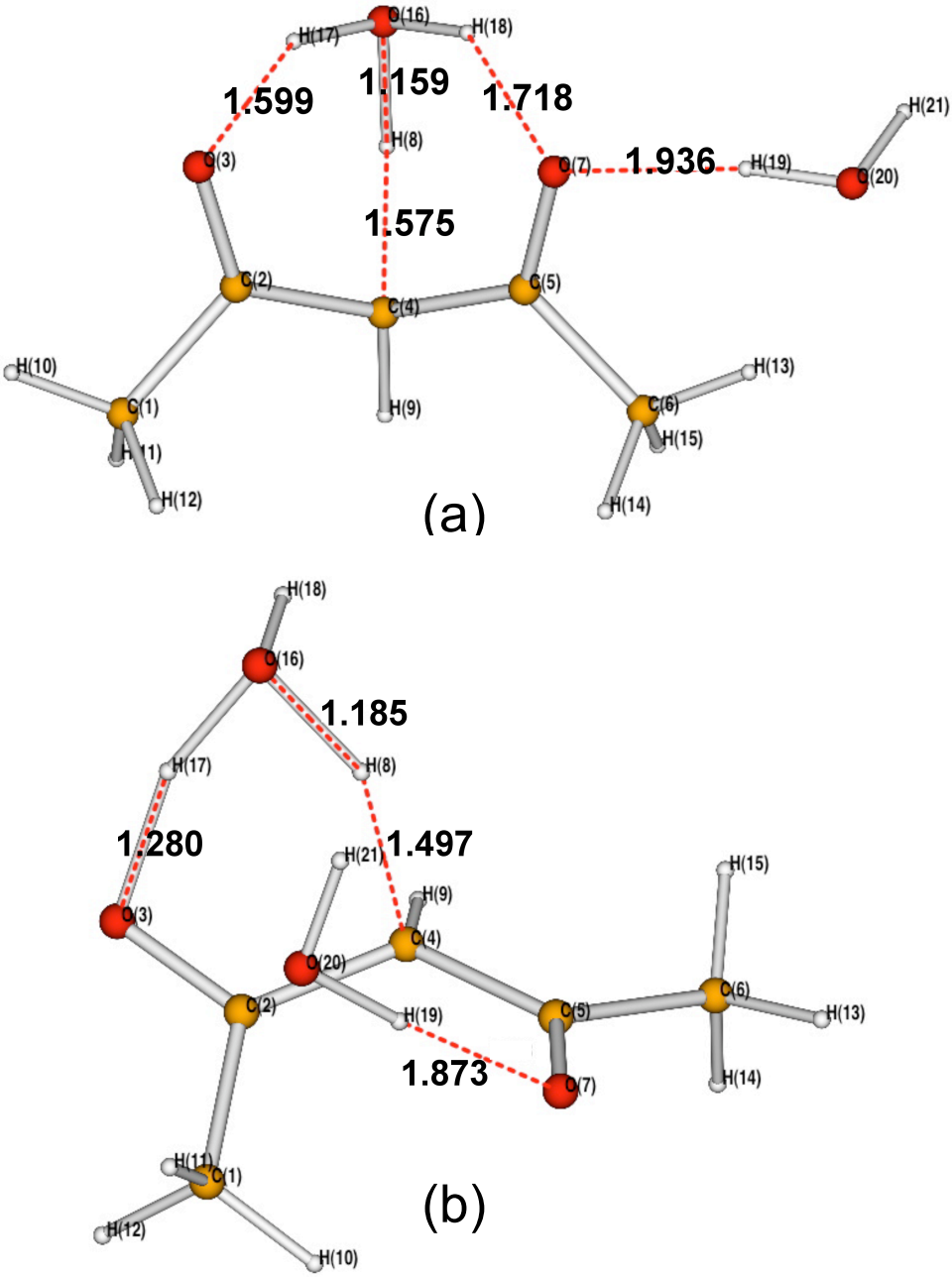

Figure S9. (a) B3LYP/6-31G* transition state (TS) structure of dihydrated acetylacetone optimised starting from the grid point at –80/1.2 on the PES of Fig. 7. Despite located at –49.1/1.16 the structures are similar. This TS structure corresponds to a sequential mechanism, i.e. only the H_8 atom is being delivered. Subsequently H_{17} should be shuttled as well. (b) The B3LYP/6-31G* TS optimised structure starting from –60/1.2 is consistent with the nonIMHB KE in the bottom right region of Fig. 7.

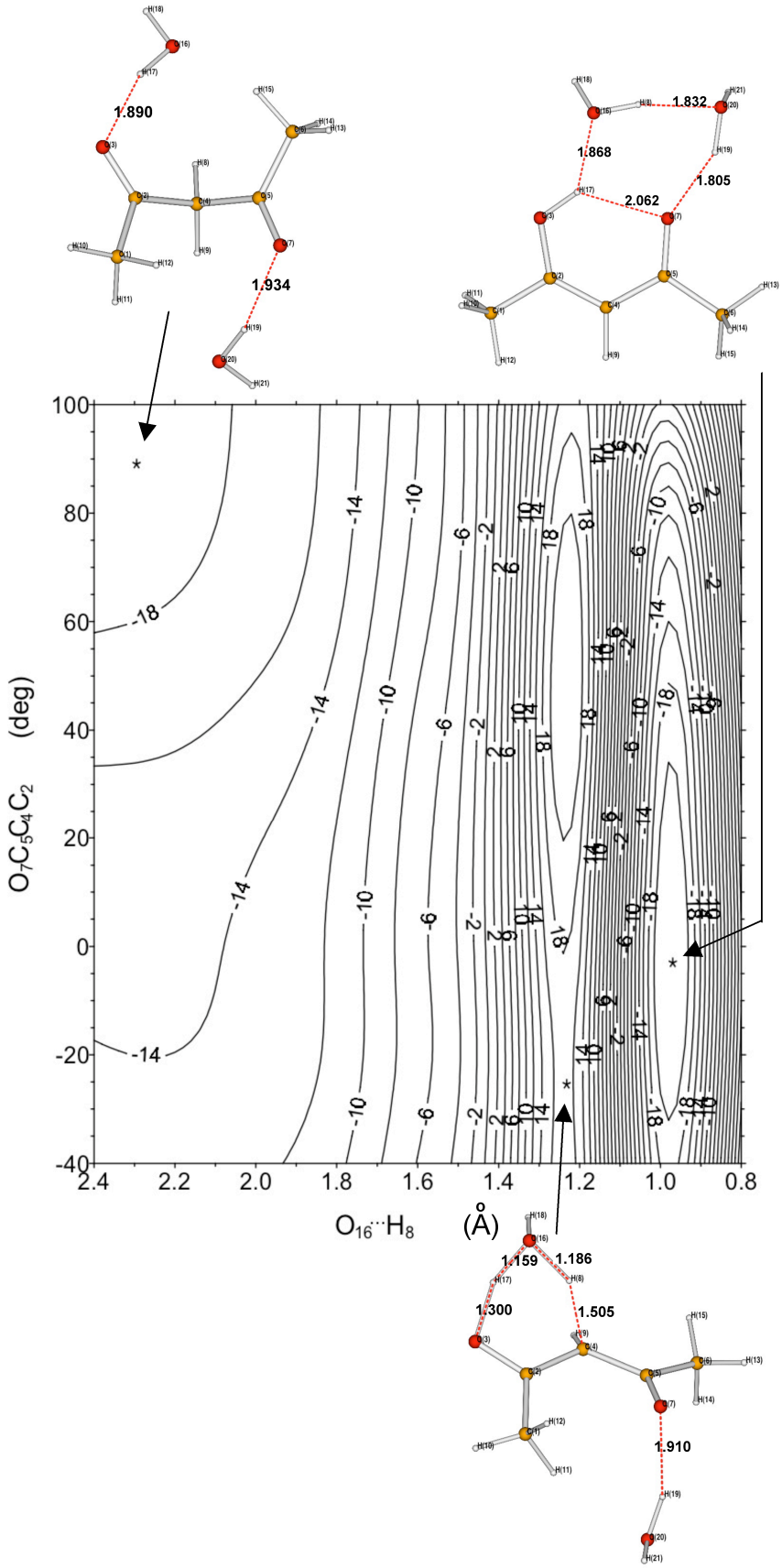

Figure S10. B3LYP/6-31G* potential energy surface of the dihydrated acetylacetone tautomerism with a number of stationary points (see text).

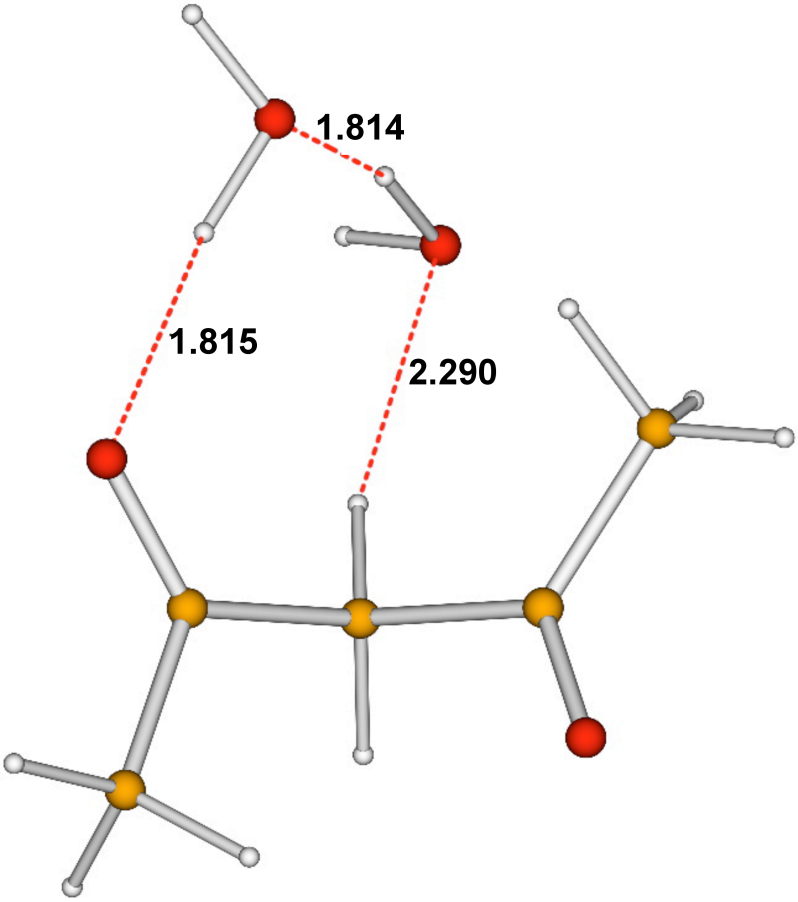

Figure S11. B3LYP/6-31G* KK optimised structure starting from waters located in the same region of space (structure close to the top left corner of Figs. 8 and 11).

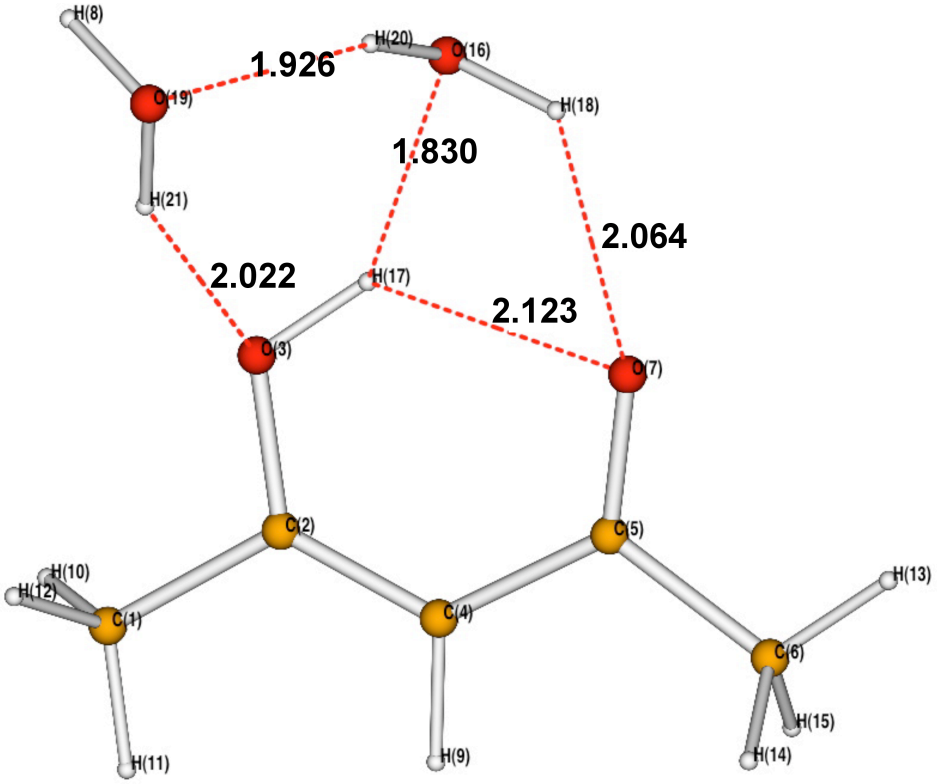

Figure S12. B3LYP/6-31G* KE optimised structure starting from the stationary point in the upper right corner of Fig. 8.

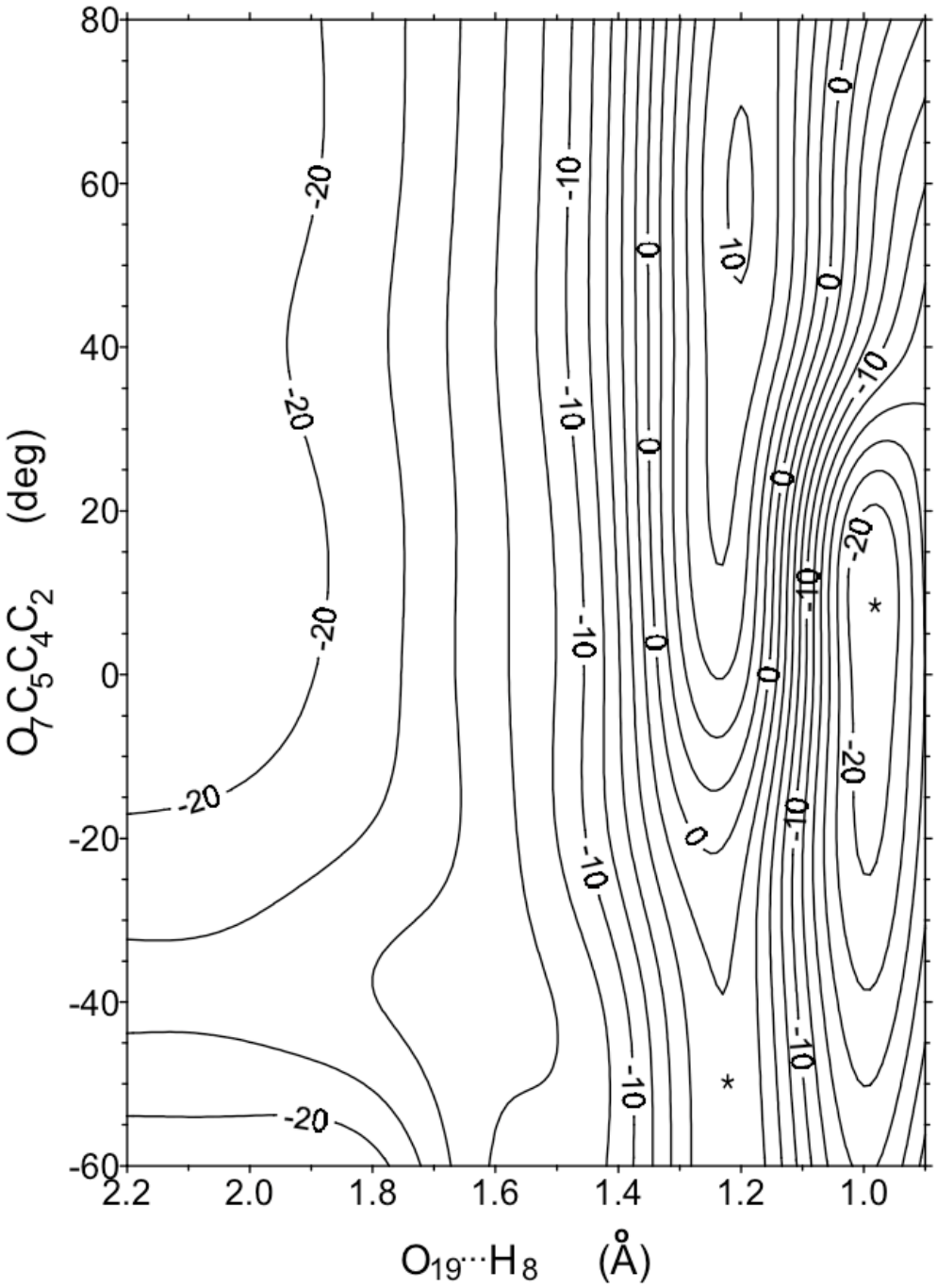

Figure S13. B3LYP/6-31G* potential energy surface resulting from a top to bottom scan (i.e. for each $O_{19}\cdots H_8$ separation, the $O_7C_5C_4C_2$ dihedral angle spans the 80 to –60° range and so on). This map is identical to that displayed in Fig. 8 (resulting from a left to right scan), but in the KE region where only the lowest minimum structure is obtained.

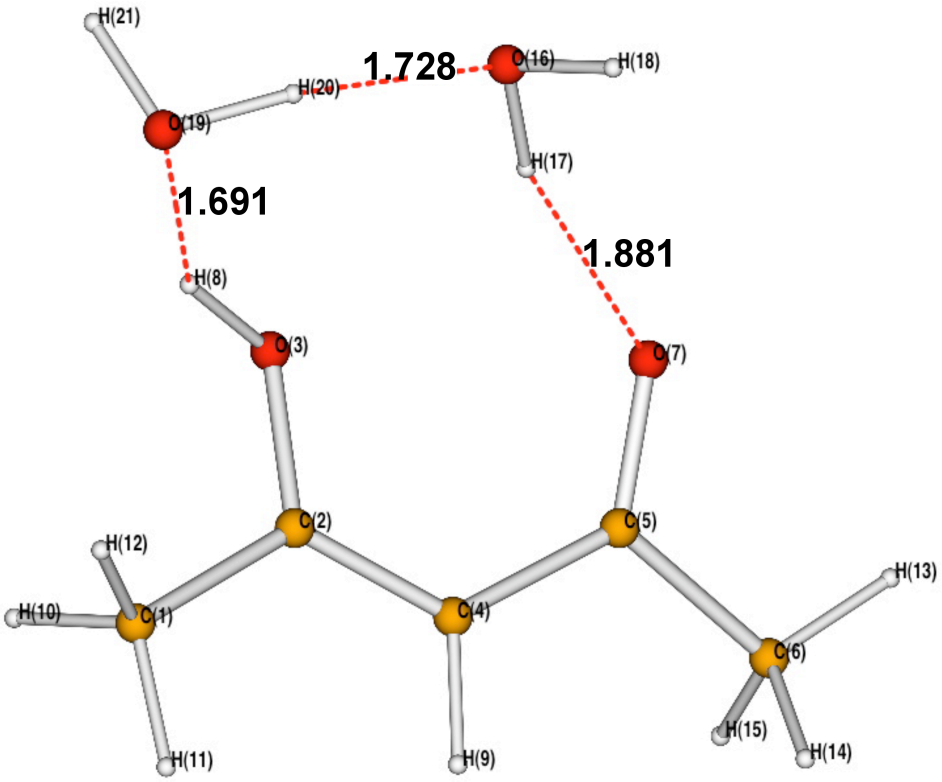

Figure S14. B3LYP/6-31G* optimised structure obtained moving from the KE to the KK structure (see text).

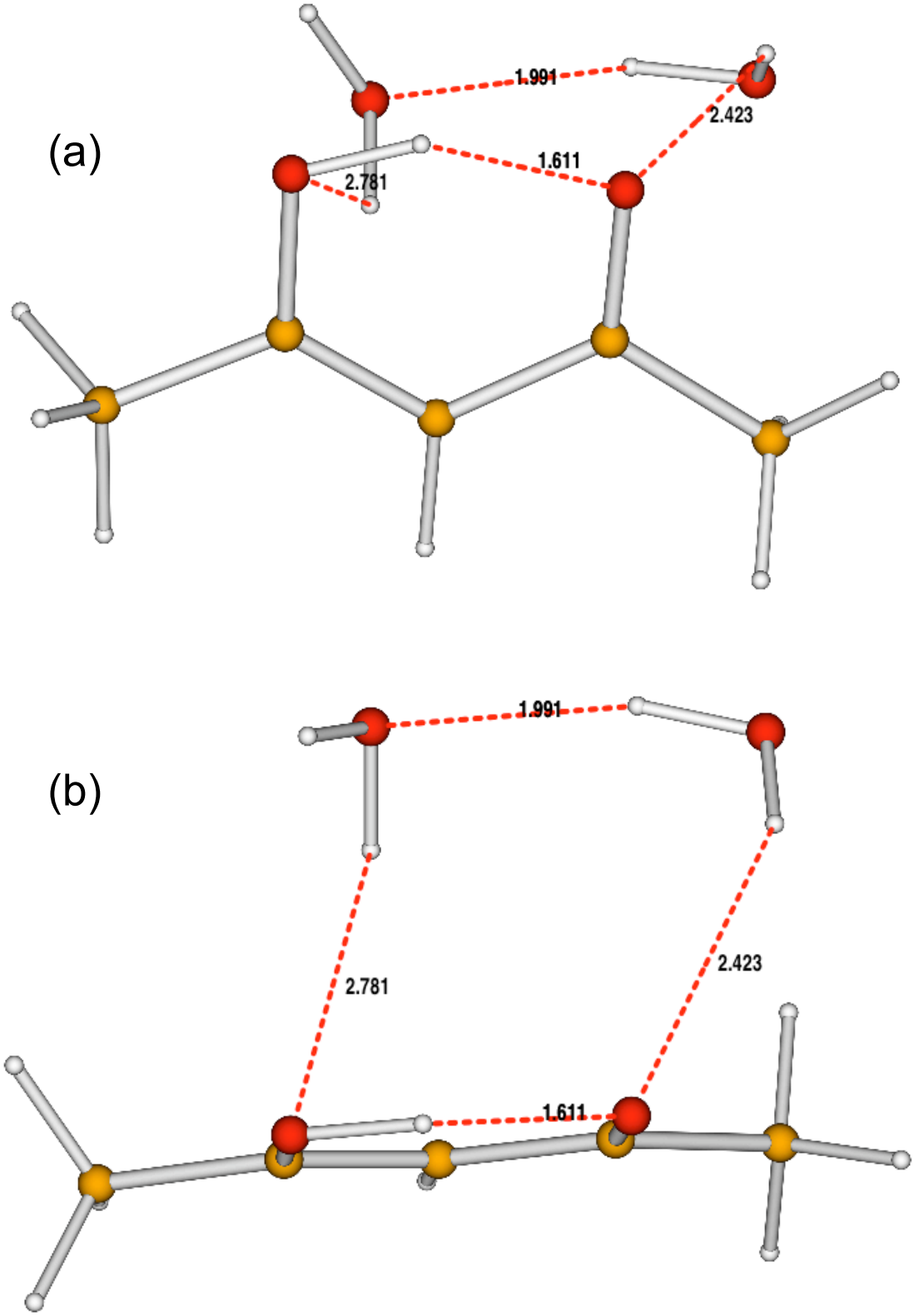

Figure S15. MP2/aug-cc-pvdz optimised structures obtained starting from the KE structure in Fig. 9: (a) front view; (b) top view.

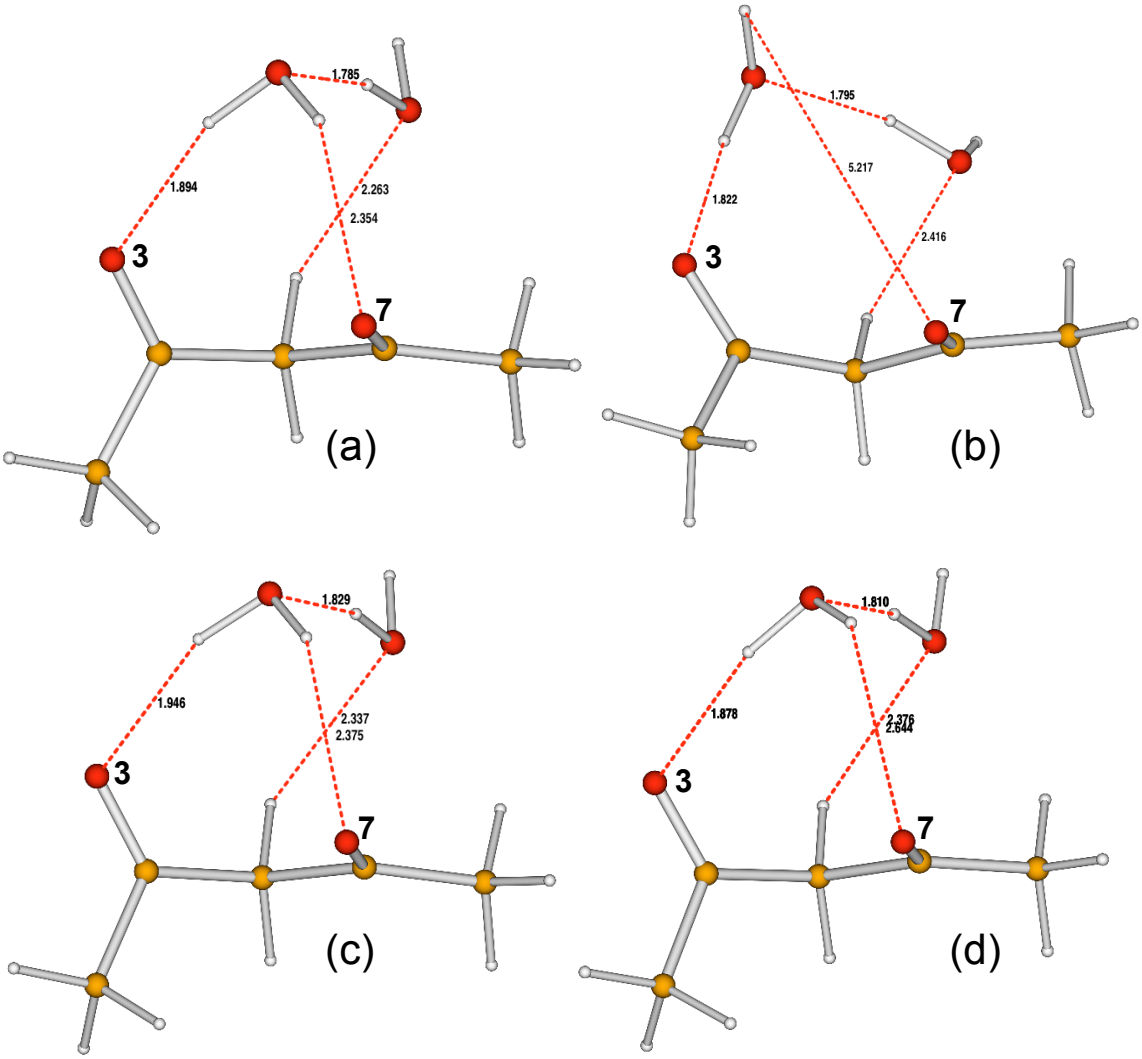

	KK+2w		KK (IEF-PCM)	KK+2w	
	B3LYP			MP2	
	6-31G*	6-31++G**	6-311++G**	6-31G*	aug-cc-pvdz
Structure	**(a)**	**(b)**	**Fig. S18c**	**(c)**	**(d)**
O_3CCC	**80.940**	**101.808**	**98.903**	**89.516**	**89.815**
O_7CCC	**–8.792**	**13.780**	**–7.084**	**–7.823**	**–4.763**
O_3CCO_7	**56.984**	**92.323**	**72.557**	**63.743**	**66.655**

Figure S16. Structures of the best KK tautomer in Fig. 9 optimised at several levels: (a) B3LYP/6-31G*; (b) B3LYP/6-31++G**; (c) MP2/6-31G*; (d) MP2/aug-cc-pvdz. Some geometric parameters are also reported and compared to those of the isolated KK tautomer embedded in IEF-PCM aqueous solution (displayed in Fig. S18c). O_3CCO_7 is the dihedral angle between the carbonyl groups

	B3LYP	
	6-31G*	6-31++G**
Structure	(a)	(b)
O_3CCC	93.211	98.926
O_7CCC	77.742	80.568
O_3CCO_7	134.197	141.598

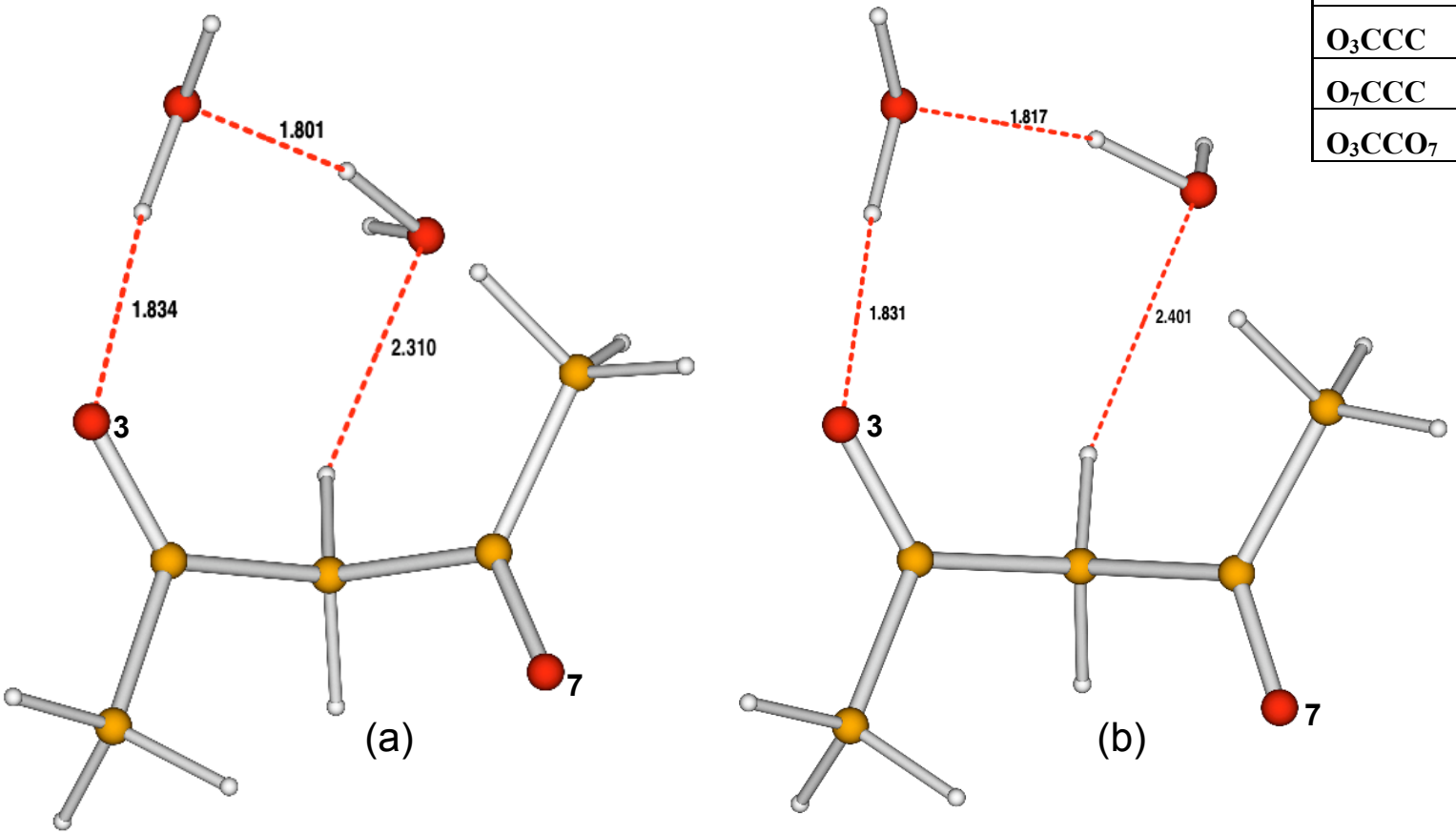

Figure S17. Structures of the KK tautomer in the top left corner of Fig. 9 optimised at two levels: (a) B3LYP/6-31G*; (b) B3LYP/6-31++G**. Some geometric parameters are also reported. O_3CCO_7 is the dihedral angle between the carbonyl groups.

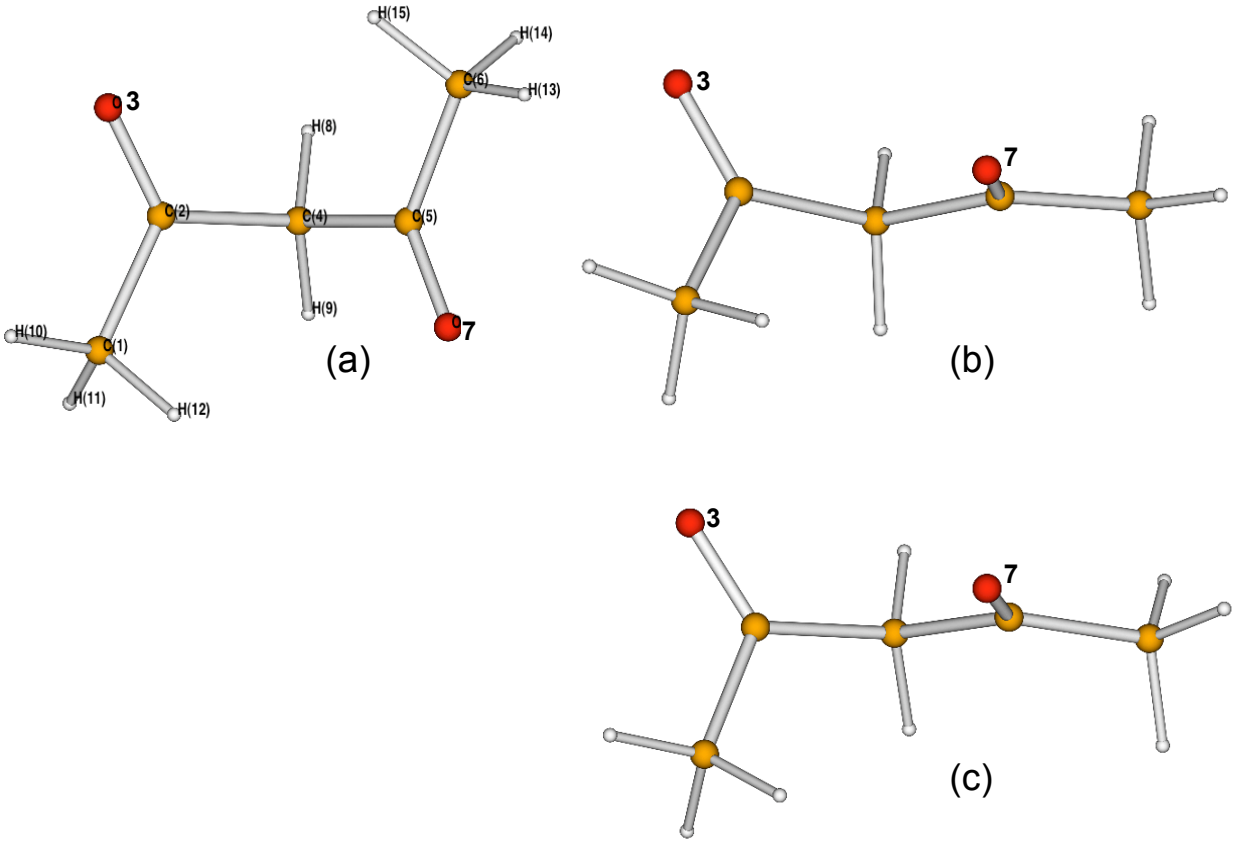

	In vacuo	IEF-PCM in water		
B3LYP	**6-31G***	**6-31G***	**6-31G***	**6-311++G****
Structure	**(a)**	**(a)**	**(b)**	**(c)**
O_3CCC	**88.238**	**89.202**	**101.665**	**98.903**
O_7CCC	**88.238**	**88.108**	**7.303**	**–7.084**
O_3CCO_7	**138.843**	**139.761**	**87.139**	**72.557**

Figure S18. Optimised structures corresponding to: (a) the lowest energy KK tautomer in vacuo (B3LYP/6-31G*); (b) the lowest energy KK tautomer in water solution (IEF-PCM/B3LYP/6-31G*, 0.39 kcal/mol more stable than the (a) structure found in water solution which is practically indistinguishable from that in vacuo); (c) the lowest energy KK tautomer in water solution (IEF-PCM/B3LYP/6-311++G**), used for the explicit solvent MC/FEP simulations. O_3CCO_7 is the dihedral angle between the carbonyl groups.